Economic Geology
Vol. 97, 2002, pp. 1779–1794

Shallow Three-Dimensional Structure from Two-Dimensional Crooked Line Seismic Reflection Data over the Sturgeon Lake Volcanic Complex

MLADEN R. NEDIMOVIĆ[†,*] AND GORDON F. WEST

Geophysics Laboratories, Department of Physics, University of Toronto, 60 St. George St., Toronto, Ontario M5S 1A7, Canada

Abstract

In principle, partial three-dimensional structural information can be obtained from two-dimensional crooked line seismic reflection data by processing the traces as swath three-dimensional data, but this potential has rarely, if ever, been fully exploited. Here, we apply procedures newly designed for this purpose to mining exploration data from a high-resolution, two-dimensional crooked line survey over a part of the Sturgeon Lake Archean greenstone belt in northwest Ontario, Canada. We then examine the results in the light of geologic data based on about 20 years of mining activity in the immediate area. The area appears highly reflective, even when using standard two-dimensional data-processing methods. But because geologic dips in the section are typically steep and the majority of viewable contact surfaces do not lie directly below the processing and acquisition lines, special data-processing procedures have been essential.

Despite appreciable background noise in the constructed images owing to the limitations of the crooked line data set, a large variety of reflection events are quite clearly positioned in three dimensions. The acquisition and processing lines run northeast-southwest, and most of the observed reflection events strike approximately east-west and dip northward. In the upper 1.5 km, they correlate well with expected layering of the mafic-felsic volcanic rocks, and in the vicinity of the Cu-Zn volcanogenic massive sulfide deposit at Lyon Lake, they agree well with information from drilling. The three-dimensional processing has successfully imaged an ore-controlling thrust fault at the Lyon Lake deposit, contacts within the volcanic pile (including the top of the Beidelman Bay subvolcanic intrusive complex), and fold structures in the volcanic stratigraphy. The results suggest that simple three-dimensional seismic surveys of limited offset and azimuth range may be sufficient for imaging structures in this type of geologic environment.

Introduction

DURING the past two decades, the seismic reflection method has evolved from a means of mapping relatively simple and continuous lithologic interfaces into a general method that commonly can image rock physical-property contrasts of almost any geometric complexity to within wavelength-related resolution limits. Many improvements in methodology have contributed to this progress, such as better field instruments and advanced image reconstruction techniques. However, the advance has principally come from so-called three-dimensional seismic surveying. In the three-dimensional method, seismic source points are distributed throughout the study area and each source is observed by a large, areally distributed array of receivers. This distribution contrasts with that of standard two-dimensional methods where source and receiver points are positioned along individual profiles. Three-dimensional seismic data has had an enormous effect in the exploration for petroleum in complex sedimentary structures. It has also led to a number of successful experiments in imaging structures in crystalline igneous-metamorphic terranes (e.g., Milkereit et al., 2000; Pretorius et al., 2000). Here, the physical-property contrasts between different lithologies tend generally to be weaker than in sedimentary basins, and the geometric shapes of the lithologic contacts are more complex.

In ore prospecting, geophysical methods such as magnetic, gravity, electrical, and electromagnetic techniques have proven themselves extremely useful. However, the spatial resolution and detection capabilities of these methods decrease proportionally with increasing depth. The new seismic three-dimensional capabilities are exciting for improved resolution at depth, but the cost is high. Therefore, it is crucial to determine if some of the improved capability can be retained while using two-dimensional data-acquisition methods, which are less expensive. At least at the crustal scale, two-dimensional seismic reflection surveys have provided much information about the largest-scale structures at great depth in the crystalline continental crust (e.g., Clowes et al., 1999).

The objective of this paper is to show how an aspect of two-dimensional surveying that is generally considered a serious hindrance to good imaging can commonly be turned to an advantage, especially in dealing with complex structures with steep dips. This aspect is the so-called "crooked line problem" in which standard two-dimensional imaging methods fail when the locations of the seismic sources and detectors follow a crooked survey profile and the lithologic interfaces are not plane (two-dimensional) surfaces. If the data-acquisition line is crooked enough, the survey can be considered as a three-dimensional survey of a narrow swath about the average profile with an irregular data density; then one can apply three-dimensional imaging techniques, albeit with some important limitations.

As an example, we present some recent results from a high-resolution two-dimensional crooked line seismic reflection survey carried out for Noranda Inc. in 1997 in northwestern Ontario, Canada. The data were recorded over the steeply north-dipping south Sturgeon Lake Archean metavolcanic sequence. This sequence hosts a number of small, polymetallic, volcanogenic massive sulfide deposits (e.g., Groves et al., 1988; Franklin, 1996). The survey was done opportunistically

[†]Corresponding author: e-mail, mladen@ldeo.columbia.edu
[*]Present address: Department of Marine Geology and Geophysics, Lamont-Doherty Earth Observatory, Columbia University, 61 Route 9W, PO Box 1000, Palisades, New York 10964-8000.

0361-0128/01/3308/1779-16 $6.00

for experimental purposes in conjunction with crustal-scale seismic reflection surveys being recorded nearby by Lithoprobe as part of its western Superior transect (White et al., 1997). The data were recorded at high resolution, 40 m shot spacing, and 20 m receiver spacing, and high-frequency reflections were observed on shot records. However, initial attempts to image structures by using two-dimensional processing methods, particularly at times shorter than 0.5 s (~1.5 km penetration depth), were not successful because of the crooked line problem.

Several authors have addressed the crooked line problem in two-dimensional seismic data processing, and some have tried to extract three-dimensional structural information from the crooked line data (Larner et al., 1979; Du Bois et al., 1990; Wang and West, 1991; Kim et al., 1992). However, the standard two-dimensional approach to data imaging remains entrenched. In this approach, a smooth or straight processing and slalom line is chosen and the data traces are binned and processed as if they were acquired along this profile. Unfortunately, this approach is ineffective whenever the reflecting geologic structures have substantial (say >15°) and/or variable components of crossdip (dip across the survey profile) and where the true source and receiver positions wander several seismic wavelengths laterally about the chosen processing profile.

Recently, we have described two alternative procedures for more accurate extraction of local three-dimensional structure from two-dimensional crooked line survey data (Nedimović and West, 1999, 2000). The first we call an "optimum crossdip stack." The final product of this procedure is an optimum crossdip section (image or stack) plotted over the corresponding crossdip color map. The optimum crossdip section is a two-dimensional seismic image superior to the standard two-dimensional stack because it is formed by taking into account the local reflector crossdip when one stacks (averages) seismic signals reflected from the same subsurface area. Standard two-dimensional sections are formed assuming that the reflectors do not dip across the survey profile. A seismic procedure called "three-dimensional poststack (after stack) migration" can be used to position the reflection events imaged by the optimum crossdip stack to their true subsurface locations. In the second procedure, the original data traces are migrated prestack (before stack) directly into a three-dimensional volume. This latter process has greater intrinsic imaging potential than the first, but it is computationally extremely cumbersome and time consuming.

Despite the positive aspects of the above developments, neither proposed method can overcome the fundamental limitations of any swath three-dimensional survey: first, the positions of the source and receiver survey points must be sufficiently distributed in the cross-line direction to prevent ambiguity in the location of the reflection points; and second, without full surface coverage, the data set may be missing many of the source and receiver locations that are required to obtain a Snell's law reflection from all possible reflection surfaces. Without complete surface coverage, reflectors that are not facing the survey line will remain invisible. We refer to the first problem as the "sufficient aperture" problem and to the second as the "viewpoint limitation."

In this paper, we show how the proposed methods work in three-dimensional imaging of reflectors under and near the Sturgeon Lake seismic profile. We focus our work largely on the economically most interesting part of the crust, the upper kilometer or so. First, we study the P-wave velocity structure and then produce the optimum crossdip stack. The large-scale velocity trends are small; velocity increases only a few hundred meters per second in the top 9 km. The optimum crossdip stack reveals that most of the imaged structure is not located below the processing and acquisition lines, thus requiring application of specialized three-dimensional imaging procedures to the crooked line data. Furthermore, the optimum crossdip stack does not image the upper 1.5 km or so (~0.5 s) and was mostly used for the large-scale geologic interpretation and to design the output volumes for the subsequently applied three-dimensional prestack migration.

Geology of the Survey Area

The Sturgeon Lake greenstone belt is one of many deformed metavolcanic sequences situated in the middle of the 900-km-long, 150-km-wide Wabigoon granite-greenstone subprovince of the Archean Superior province, Canada (Fig. 1). The seismic survey line obliquely crosses the central part of the southern Sturgeon Lake belt (Fig. 2). The area has low relief and is largely covered by glacial deposits, most of which are less than 10 m thick. Owing to glaciation, bedrock is largely unweathered. Geology has been mapped from sparse outcrop, numerous exploration drill holes, and the mine workings (e.g., Trowell, 1983; Blackburn et al., 1991).

The greenstone belts of the central Wabigoon subprovince have irregular map outlines and lie engulfed in a sea of granitoid and gneissic rocks that seem both to host and intrude them. The intrusive complexes are predominantly composed of trondhjemite and granodiorite. The greenstones are almost uniformly of low to moderate metamorphic grade. A tripartite subdivision can be made of the granitoid rocks (Blackburn et al., 1991). In some parts of the central Wabigoon region they

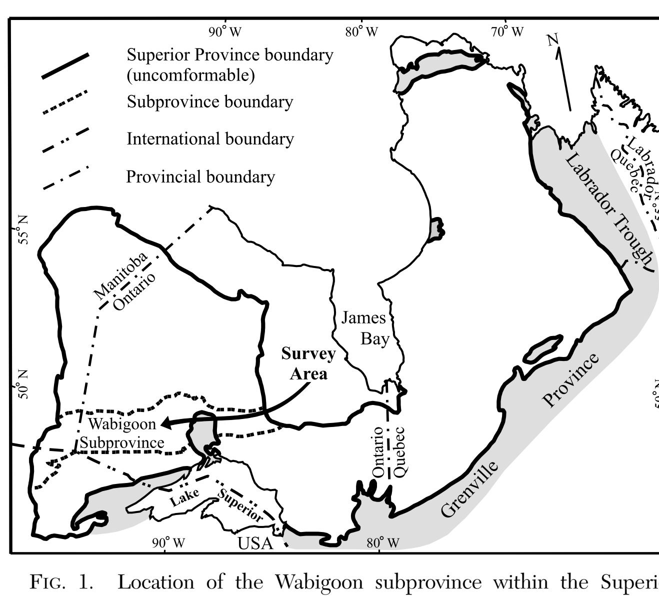

FIG. 1. Location of the Wabigoon subprovince within the Superior province.

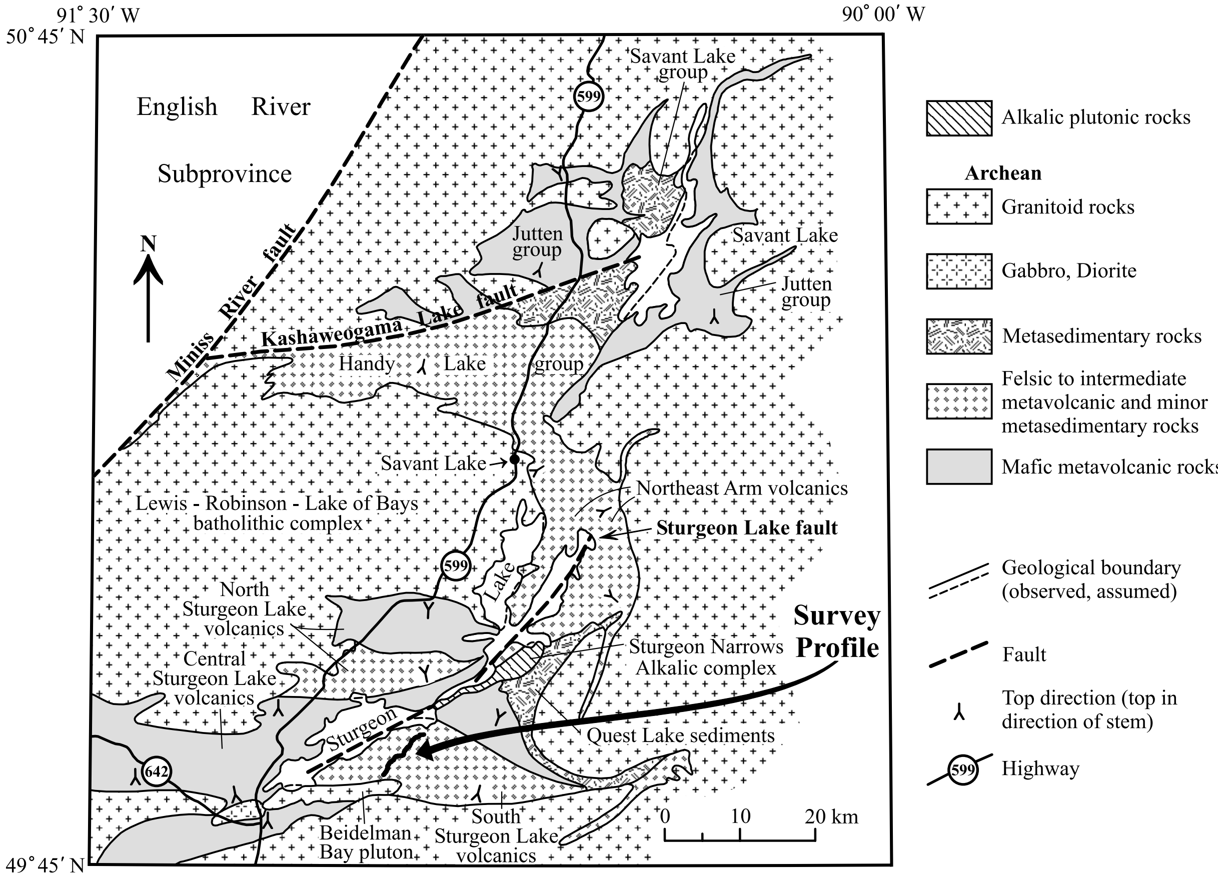

FIG. 2. Simplified geologic map of the Sturgeon Lake and Savant Lake greenstone belts (after Blackburn et al., 1991). Volcanic assemblages in the southern part of the map compose the Sturgeon Lake greenstone belt.

appear to form a basement complex underlying ~3000-Ma-old greenstones (Franklin et al., 1975), some are petrogenetically and geochronologically linked with volcanism, and most are postvolcanic and appear both marginal and internal to supracrustal belts. Some of the basement complex gneissic bodies, dated older than ~3075 Ma (Davis et al., 1988), are among the oldest in the Wabigoon subprovince.

On the basis of lithology and geographic distribution, the Sturgeon Lake greenstone stratigraphic succession has been subdivided into four assemblages composed of several volcanic cycles that can be further subdivided into formations (Trowell, 1983). All cycles contain a similar bimodal pattern of compositional variation. Lower units are mafic to intermediate metavolcanic rocks, and upper units are felsic to intermediate metavolcanic rocks. Cycle and assemblage boundaries are demarked by a hiatus in volcanism, a change in composition, and/or a period of sedimentation. Metasedimentary rocks in an assemblage are mostly clastic (e.g., sandstone, mudstone, conglomerate) and to a lesser extent chemical (e.g., chert, sulfide). Substantial subvolcanic gabbroic and ultramafic rocks commonly intrude lower mafic metavolcanic rocks, and the same intrusive material is also found extensively in the felsic to intermediate fragmental rocks and clastic metasedimentary rocks. The metavolcanic and metasedimentary rocks, mafic and ultramafic intrusions, and felsic epizonal intrusions all are metamorphosed from greenschist to lower amphibolite grade.

Southern Sturgeon Lake Assemblage

The south and north Sturgeon Lake assemblages appear to form opposing limbs of a synformal structure whose east-northeast–trending axis is located south of the north shore of Sturgeon Lake (Trowell et al., 1980; Trowell, 1983). However, stratigraphic correlation between metavolcanic rocks of the two assemblages is not possible (Trowell et al., 1980; Severin, 1982). The apparent thickness of the south Sturgeon Lake assemblage exceeds 9,000 m (Trowell, 1974, 1983; Franklin et al., 1977). Franklin et al. (1977) divided this volcanic pile into three volcanic cycles, all of which are fully or partially intersected by the Sturgeon Lake seismic line (Fig. 3). From oldest to youngest (i.e., from southwest to northeast on the seismic line), they are cycle 1, cycle 2, and cycle 3. Strata in all three volcanic cycles form a homocline that approximately faces toward the north with a steep dip. The boundary region between the lower two cycles (1 and 2) is a major thrust fault (Fig. 3).

Cycle 1

Cycle 1, subdivided by Trowell (1983) into five formations (A, B, C, D, and E), has been reinterpreted by Morton et al.

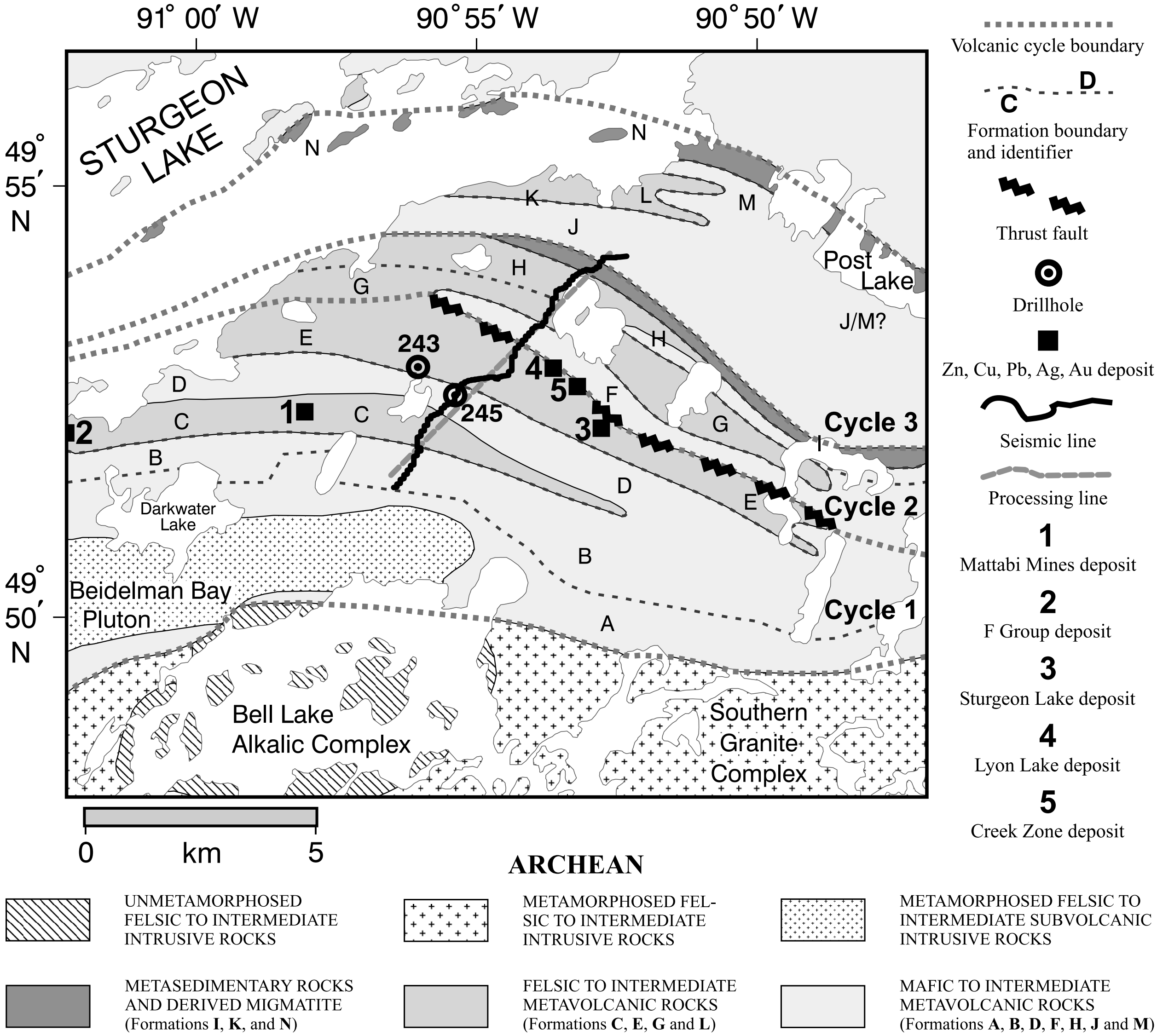

FIG. 3. Geologic map of the southern Sturgeon Lake assemblage showing the acquisition and processing lines. The composition of volcanic cycles and formations is described in the text. The map is based on data from Ontario Geological Survey Map 2442 (1980); Trowell's chart A (1983); Dubé et al. (1989), and Morton et al. (1996); acquisition and processing coordinates for the Sturgeon Lake line; and drill hole coordinates. Relationship between systems by Trowell (1983) and Morton et al. (1996) for the area crossed by the survey is provided below. Volcanic cycle 1: formation A = precaldera volcanic complex; formation B = Jackpot Lake succession and High Level Lake succession; formations C and D = Tailing Lake succession; formation E = L succession. Volcanic cycle 2: formation F = Lyon Lake andesite; formation G = Swamp Lake succession; formation H = felsic volcanic rocks; formation I = sediments. Volcanic cycle 3: formation J = mafic volcanic rocks.

(1991, 1996) as comprising precaldera volcanic rocks and the Sturgeon Lake caldera complex. The precaldera volcanic rocks (formation A in Figure 3) represent part of a large subaerial-subaqueous shield-type volcano composed of a thick sequence of basalt flows, scoria-tuff cone and debris flows, and minor amounts of interlayered rhyolitic lava flows and pyroclastic fall deposits. The Sturgeon Lake caldera complex (formations B, C, D, and E in Fig. 3) is subdivided into five volcanic successions. Massive to well-bedded pyroclastic flow and fall deposits of the Jackpot Lake succession overlie the precaldera volcanic rocks. These aphyric ash tuff deposits are 50 to 300 m thick. The High Level Lake succession is represented by two units. The 80- to 900-m-thick and poorly sorted mesobreccia and megabreccia deposits immediately overlie the precaldera volcanic rocks or the Jackpot Lake pyroclastic units; they are composed of block- and lapilli-size clasts of mafic and felsic volcanic rocks. The 50- to 350-m-thick ash flow tuff deposits are mostly composed of quartz-crystal–rich rhyolite and pumice-rich dacite. Some 60 to 400 m of subaqueous debris flow deposits and bedded epiclastic rocks of the Tailings Lake succession overlie the High Level Lake succession. Locally, the debris flow deposits and associated sediments are separated by dacitic ash tuffs and by dacitic to andesitic lava flows. The debris flow deposits are mostly composed of precaldera mafic volcanic and High Level Lake succession ash flow tuff clasts. The felsic ash tuffs are aphyric and fine grained, and the lava flows range from massive to amygdaloidal and brecciated. East of Darkwater Lake, ash flow tuffs of the Mattabi succession directly overlie the Tailings Lake succession. Predominantly, these are well-bedded quartz-crystal–rich flows, 150 to 1,200 m thick. They represent the most voluminous eruptive event within the caldera. Late caldera volcanism is represented by rocks of the L succession, which range from quartz- and quartz-plagioclase–bearing pyroclastic deposits through plagioclase-phyric lava flows, and a major dome that contains sedimentary sequences including iron formation. The entire succession is 250 to 1,200 m thick.

Cycle 2

Cycle 2 is composed of four formations: F, G, H, and I (Trowell, 1983). Formation F is represented by interlayered massive to amygdaloidal basaltic to andesitic sheet-flows and fragmental rocks with possible intrusive equivalents (Dubé et al., 1989). Formation G consists of fine-grained, finely quartz-porphyritic, massive homogeneous felsic metavolcanic rocks. Formation H is made of intercalated mafic to intermediate flows with minor tuffs and felsic fragmental rocks. Rocks of formation I are clastic metasedimentary rocks (wacke, mudstone, siltstone, conglomerate) and were interpreted by Trowell (1983) to indicate a substantial hiatus in volcanism. This notion is further supported by rare earth element, major element, and selected trace element data (Campbell et al., 1981, 1982; Davis et al., 1985) as well as by subsequent U-Pb zircon dating (Davis et al., 1985). Chemically, the felsic metavolcanic rocks of the lower two cycles (1 and 2) are very similar to each other and distinctly different from those of the upper cycle (3). Geochronology indicates that the felsic metavolcanic rocks of volcanic cycles 1 and 2 are of nearly the same age (2735.5 ± 1.5 Ma) and significantly older than felsic metavolcanic rocks of cycle 3 ($2717.9^{+2.7}/_{-1.5}$ Ma).

Cycle 3

Cycle 3 is composed of five formations: J, K, L, M, and N (Trowell, 1983). Formation J consists of massive, pillowed, and amygdaloidal mafic flows. Formation K comprises wacke and carbonaceous and sulfidic mudstone. Intermediate to felsic fragmental rocks of formation L are epiclastic in origin. Formation M is composed of massive, pillowed, amygdaloidal, and finely feldspar-porphyritic mafic volcanic flows. Formation N overlies the south Sturgeon Lake assemblage and is composed of clastic metasedimentary rocks (debris flow, conglomerate, thickly bedded wacke-siltstone, and iron formation).

Related Intrusions

Because strata in the south Sturgeon Lake assemblage dip toward north, all structures lying at its base probably also face northward and may possibly be imaged from the survey line. These could include, for example, the southern contact between the metavolcanic rocks and the intrusions, as well as the contacts within somewhat concordant intrusive rocks. The surface extension of these intrusions is represented by a few distinct geologic units (Fig. 3): the Beidelman Bay pluton, the Bell Lake alkalic complex, and the Southern granitic complex.

Beidelman Bay pluton

The Beidelman Bay pluton is situated within the precaldera rocks of the volcanic cycle 1 and is variously massive, foliated, and sheared. Its boundary is characterized by locally intense brecciation. Five different magmatic phases have been identified in this intrusion that differ in morphology, composition, and time of occurrence, but are all tilted steeply to the north (Galley et al., 2000). All phases of the Beidelman Bay intrusion have undergone upper greenschist grade to lower amphibolite grade regional metamorphism. Most of the Beidelman Bay intrusion, including the part shown in Figure 3, consists of fine- to medium-grained biotite trondhjemite. The very similar chemical composition of this part of the intrusion and the overlying felsic rocks of the first two volcanic cycles suggests that they are comagmatic (Campbell et al., 1981; Davis et al., 1985; Galley et al., 2000). U-Pb dating puts the age of at least part of the intrusive complex at $2733.8^{+1.4}/_{-1.3}$ Ma, only nominally younger than the metavolcanic rocks of the first two cycles (2735.5 ± 1.5 Ma).

Southern granitic complex

The Southern granitic complex in the Bell Lake area is composed of amphibolitic mafic metavolcanic rocks extensively intruded by granodiorite-trondhjemite that forms arrays of concordantly layered sheets. Away from the Bell Lake area, the granodiorite-trondhjemite becomes strongly foliated to banded or gneissic and contains only sparse local amphibolite xenoliths.

Bell Lake alkalic complex

The latest igneous activity in the area was probably the intrusion of the Bell Lake alkalic complex, which is mostly composed of equigranular and porphyritic monzonite, syenite, and diorite. This elliptical stock intrudes the Southern granitic complex. The contacts between the two intrusions are variously chilled, faulted, and gradational. Intrusion breccia locally occurs along the margin of the stock, and the configuration of the contact at depth is speculative.

Mining Activity

Despite a long history of exploration for gold, the most economically valuable ores found in the Sturgeon Lake greenstone belt are polymetallic base-metal massive sulfides. Several Zn-Cu–rich orebodies were discovered in the south Sturgeon Lake assemblage in a short period of time from 1969 to 1972. Geophysics played a major role in their detection (Severin, 1982). Magnetic anomalies obtained by an airborne magnetic survey in 1969 were later probed by a variety of ground geophysical surveys (e.g., induced polarization, electromagnetic, magnetic, gravity). The most promising anomalies were tested by drilling.

All of the orebodies (Fig. 3) were located within or at the top of the clastic felsic metavolcanic rocks of the volcanic cycle 1 (Severin, 1982). Several authors (e.g., Franklin et al., 1977; Campbell et al., 1981; Trowell, 1983) believe that the Beidelman Bay pluton played an important role in the generation of the sulfide deposits. Rare earth and other trace element characteristics are similar in parts of the subvolcanic sill and the overlying ore-bearing felsic metavolcanic rocks (Campbell et al., 1981; Galley et al., 2000). This similarity suggests that the sill could have been either the magma chamber that fed the felsic volcanism of cycle 1 (Campbell et al., 1981) or a thermal source for the hydrothermal convection that scavenged these formations.

The first and largest discovered deposit (1969) is the Mattabi orebody. Franklin et al. (1975; Franklin, 1996) report that it contained 11.4 Mt of 8.28 percent Zn, 0.74 percent Cu, 0.85 percent Pb, 104.0 g/t Ag, and 0.2 g/t Au. The smallest discovery (1970) was the F group deposit with 0.34 Mt of 9.51 percent Zn, 0.64 percent Cu, 0.64 percent Pb, 60.4 g/t Ag, and 0.2 g/t Au (Franklin, 1996). The Sturgeon Lake deposit was also discovered in 1970 and had 2.07 Mt of 9.17 percent Zn, 2.55 percent Cu, 1.21 percent Pb, 164.2 g/t Ag, and 0.6 g/t Au (Severin, 1982; Franklin, 1996). The Lyon Lake deposit was discovered in 1971 and had 3.94 Mt of 6.53 percent Zn, 1.24 percent Cu, 0.63 percent Pb, 141.5 g/t Ag, and 0.2 g/t Au (Harvey and Hinzer, 1981; Franklin, 1996). The Creek Zone deposit, discovered in 1972, had 0.91 Mt of 8.80 percent Zn, 1.66 percent Cu, 0.76 percent Pb, 141.5 g/t Ag, and 0.6 g/t Au (Harvey and Hinzer, 1981; Franklin, 1996).

The F group, Mattabi, Lyon Lake, and Creek Zone deposits were exploited by what is today Noranda Inc., and the Sturgeon Lake volcanogenic massive sulfide deposit was exploited by Falconbridge Copper Ltd. The Sturgeon Lake, F group, and Mattabi deposits were depleted in 1981, 1984, and 1988 respectively, whereas production at the Lyon Lake and Creek Zone deposits stopped in 1991 (Morton et al., 1996). At the time that the high-resolution Sturgeon Lake seismic reflection line was acquired (1997), all mining activity in the area had ceased. The seismic data were collected to explore the feasibility of revealing structural relations at depth and to search for deeper ore targets in this important base-metal–rich area.

Survey Parameters and Data Processing

The Sturgeon Lake line seismic reflection data were acquired by using a fixed recording spread 7.84 km long with 393 active receiver groups spaced every 20 m. A total of 182 shots (0.5 kg explosive charges in holes drilled to bedrock) were fired along the profile every 40 m. After each shot, vertical ground motion was sampled at a 1 ms rate for 3 s by all receivers. Source-generated signal in the recordings has a wide bandwidth from several Hz to more than 300 Hz. The data are of very good quality and have a high signal/noise ratio. Surface waves were not a serious problem. Data was processed according to the procedures described by Nedimović and West (1999, 2000). A summary of the processing flow is presented in Appendix A.

Results and Interpretation

Velocity structure

Seismic reflection data are recorded in time. Processing of seismic data, conversion of the obtained images into depth sections, and in particular depth imaging via prestack migration all require a good knowledge of wave velocities in the study area. The P-wave velocity model for the Sturgeon Lake line area was determined from well logs and the seismic data. Densely sampled (0.5 m) data sets were available for drill holes 243 and 245. In addition to P-wave velocity, the drill holes were also logged for density. P-wave reflection imaging, used in this study, is directly dependent on the magnitude of change in acoustic impedance (the product of density and P-wave velocity) at lithologic boundaries. Generally, the greater the change in acoustic impedance, the stronger the reflections. Density and P-wave velocity logs are shown in Figure 4 together with the resulting log of acoustic impedance and summary core logs. Drill hole 243 is located about 1 km northwest of the seismic line, and drill hole 245 is on the line (Fig. 3). The holes dip to the south and were logged to total depths of 1,200 and 600 m, respectively.

The logs in Figure 4 show that the P-wave velocity can vary up to several hundred meters per second between consecutive measurements. Although some of this variation may be measurement error, most of it is due to local variation within the penetrated rock, which is heterogeneous and possesses well-developed layering typical of this type of volcanic succession. Most of the penetrated materials are felsic rocks (e.g., rhyolite flows, tuffs, agglomerates, breccias, rhyodacite and dacite flows and tuffs, aplite dikes), with a minor intermediate component (andesite). The large changes in velocity among these lithologies cause strong variations in the acoustic impedance (Fig. 4) which, in turn, causes the reflection energy in the top part of the raw seismic data.

The velocity log for drill hole 243 indicates a mild inverse velocity-depth trend. Statistical analysis applied to the data shows that more than 75 percent of all measurements lie within a 400 m/s range that shifts from 5.8 to 6.2 km/s for the upper 600 m down to 5.6 to 6.0 km/s for the lower 600 m. The velocity log for drill hole 245 shows somewhat greater dispersion. Nevertheless, more than 60 percent of the measurements of the full 600 m depth range lie within the same 5.8 to 6.2 km/s window as the drill hole 243 data.

Density logs for both drill holes (Fig. 4) show values in the range from 2.65 to 2.90 g/cm^3, as expected for fresh felsic to mafic material of low porosity. As with the velocities, densities generally decrease slightly with depth. This trend reverses below about 1,000 m. The simplified summary of descriptive core logs for both drill holes (Fig. 4) does not indicate any systematic change in lithology that could explain the small systematic decrease with depth of both velocity and density. However, most of the variations in the physical property logs below 100 m are likely related to changes in local mineralogic composition and/or to the degree and type of interbedding (i.e., number and thickness of layers).

Refraction and reflection arrival times were both used to obtain P-wave velocities from the seismic data. First breaks were picked to estimate the near-surface velocity structure, whereas reflections were studied to estimate velocities at deeper horizons. Results obtained from the first arrival data are presented in Figure 5. They show a few meters thick and slow (<1 km/s) layer of unconsolidated glacial drift overlying the bedrock with velocities in the range of 5.6 to 6.2 km/s. The refraction interpretation model generally agrees with log results but suggests slightly lower velocities in the uppermost few hundred meters of the bedrock, perhaps owing to some relict weathering or near-surface fracturing. However, the

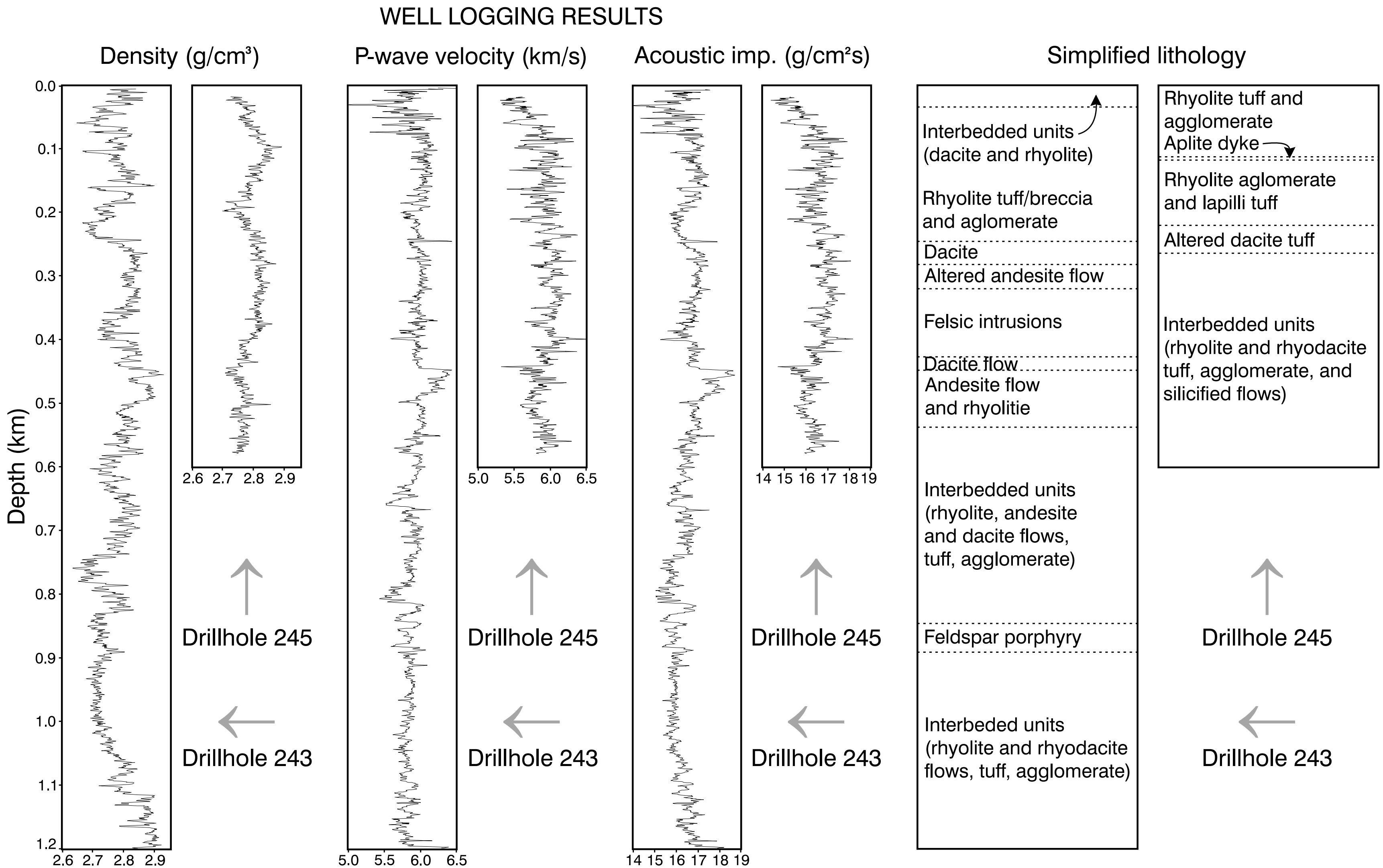

FIG. 4. P-wave velocities, densities, and acoustic impedance of the shallow structure in the Sturgeon Lake line area obtained from data collected by well logging. Simplified summary drill logs accompany the physical property logs. The plots show strong variation in acoustic impedance (product of density and P-wave velocity) throughout the drill holes, and they indicate that detailed reflection imaging in this area is likely to be successful. Note that the resolution of the logs is higher than that which can be sensed seismically. The seismic spatial resolution for signals band-limited at 100 Hz and medium velocities of about 6.0 km/s is about 15 m (5 m at 300 Hz).

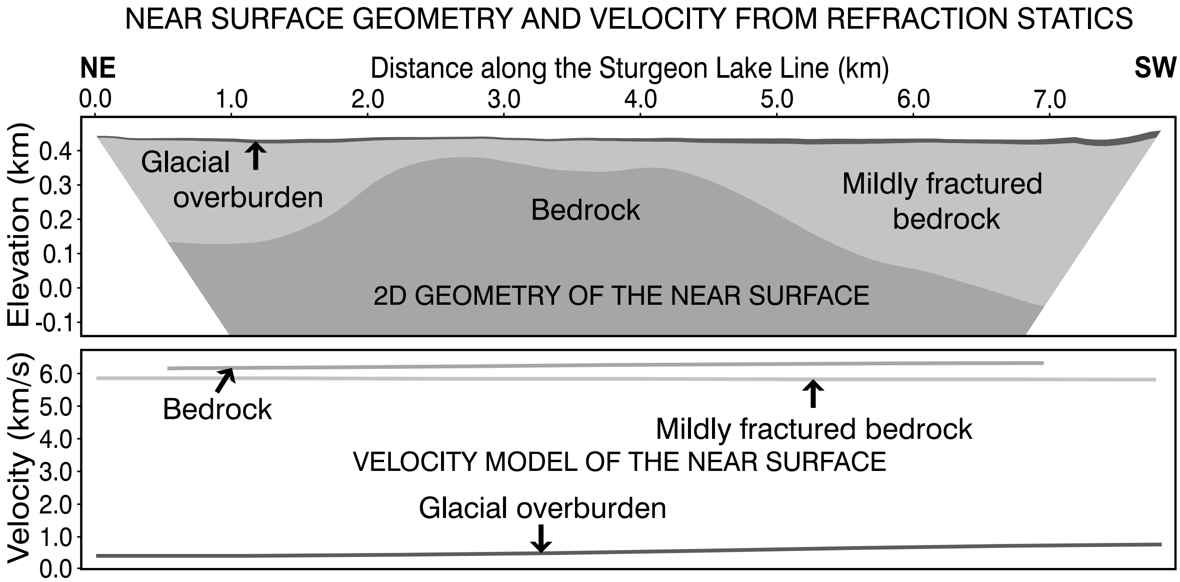

FIG. 5. P-wave velocities of the shallow structure along the Sturgeon Lake line obtained from first arrivals are illustrated by a model of the near surface. The plot shows that the glacial overburden along the seismic line is 2 to 20 m thick. P-wave velocities within the overburden are significantly lower (<1 km/s) than the velocities within the bedrock (~6 km/s), which appears to be fractured at the top.

slightly lower upper bed-rock velocities in the refraction model could also be caused by a misinterpretation of systematic lateral variations in velocity that correlate with the steeply dipping volcanic lithology.

An accurate determination of velocity structure from the reflection arrivals from crystalline rocks is commonly difficult, because sharp focusing of signals along hyperbolic (normal moveout) time paths is rarely observed (Nedimović et al., 1998). The lack of focus is thought to be due to complicated shapes of reflecting interfaces and two-dimensional crooked line data acquisition. Only a simple P-wave velocity model could be extracted from the Sturgeon Lake line data. Velocities of ~6.0 km/s characterize rocks at depths of up to a few kilometers. At greater depth they become noticeably higher, gradually reaching 6.3 to 6.5 km/s at depths of 7 to 8 km. No reliable velocity estimates could be obtained from reflection data for the top kilometer or two.

Optimum crossdip stack

The optimum crossdip stack of the Sturgeon Lake line data is shown in Figure 6a. Reflected energy is pervasive in this section. The reflections recorded at late times (1.5–3.0 s, corresponding to depths of ~4–9 km) are by far the strongest events. This is not evident on Figure 6a because several amplitude-equalization processes have been applied to the data. Most of the reflection events appear to be subhorizontal along the line or to dip to the northeast, and they appear to have northwest crossdip. Therefore, the majority of the imaged reflectors lie south or southeast of the acquisition and processing lines and dip toward the north or northeast. The pattern of events varies throughout the section, and for the purpose of discussion it can be divided into three regions (Fig. 6a). The boundaries between the regions are not sharp, nor are they always clearly defined. In the deepest region, the events are largely subhorizontal. The middle region contains a pattern of overlapping and interfering horizontal and apparent northeast-dipping events in which the dipping events predominate. The shallowest region contains events with a variety of apparent dips, but gentle dips predominate. However, in the region above 0.5 s and within the few hundred meters at both profile ends, the reliability of the image is low. It is important to remember that, because of variations in crossdip, events that cross each other on the section are unlikely to actually intersect in the earth.

Any geologic interpretation of deep reflection events is naturally speculative. The apparently horizontal or mildly dipping reflections at 2.5 s (~7.5 km) and below could possibly outline the top of basement gneisses or a large batholith intruded by many subhorizontal sills (e.g., Juhlin, 1990). We believe that the groups of reflections indicated in Figure 6a as A, B, C, and D are related to the intrusive rock units shown in the southern part of the geologic map in Figure 3. At and near the surface, these sill-like intrusive bodies show shearing at their contacts and well-developed layering of various origins, and they are known to dip steeply to the north. The reflectors A, B, C, and D have strong components of both northeast in-line and northwest cross-line dip; i.e., they are the steepest north-dipping events in this section. When extrapolated to the surface, reflectors A, B, C, and D intersect the geologic map at the location of intrusive rocks of the Beidelman Bay pluton, the Bell Lake alkalic complex, and the Southern granitic complex. This observation is confirmed in the following section on three-dimensional migration where the same reflector groups are shown at their true subsurface locations in a three-dimensional image volume. The greenstones on the geologic map appear to be intruded and pushed aside by these younger intrusive rocks that are roughly concordant to each other and to the greenstones, but which

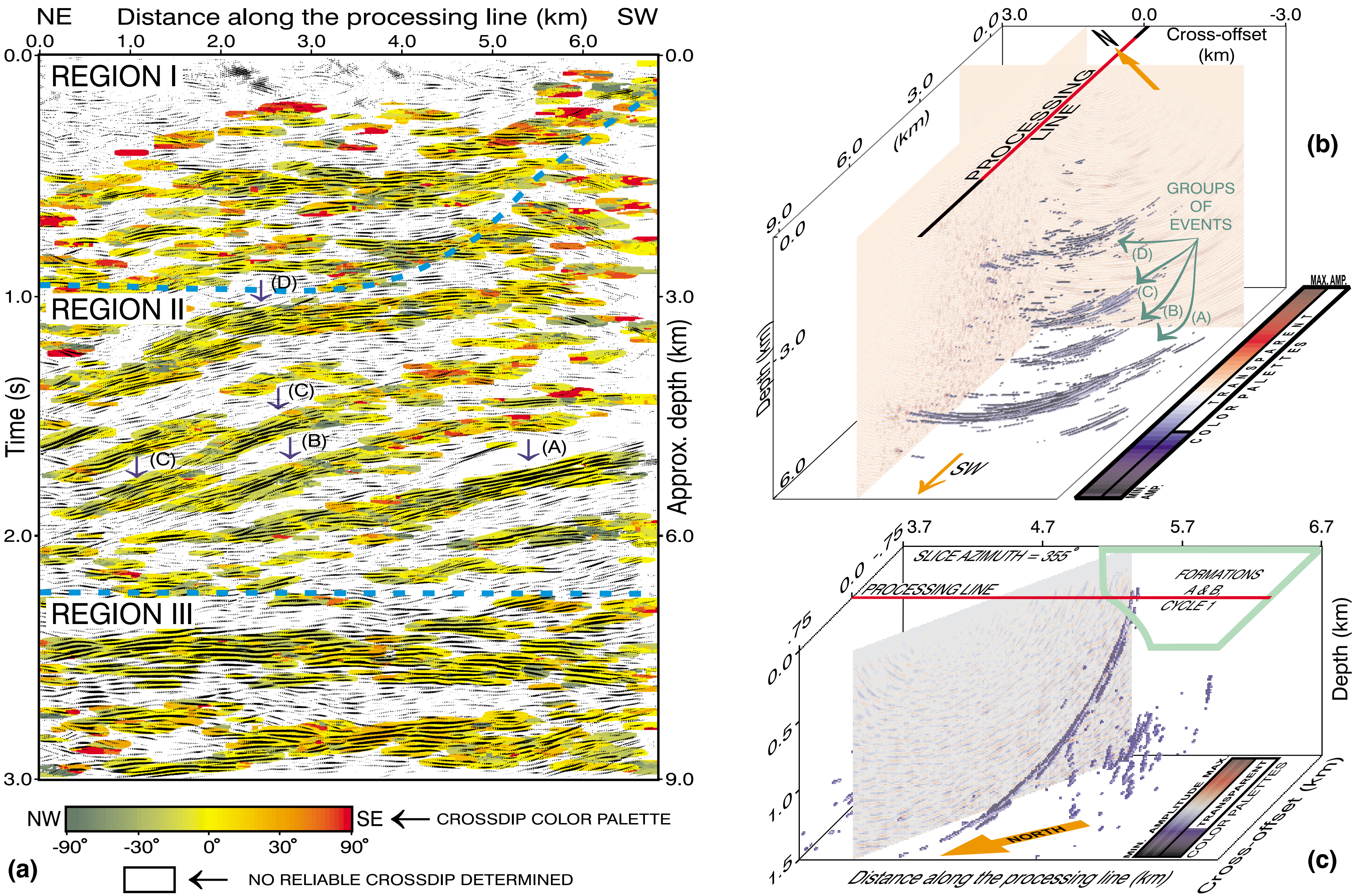

FIG. 6. Regional scale images obtained from the Sturgeon Lake line seismic data. (a) Locally optimum crossdip stack superimposed on the corresponding crossdip color map. Shades of green and red indicate the intensity of crossdip. Events that face the processing line and lie on the southeast side of it are green. Events on the northwest side are red. On the basis of the patterns observed in the optimum crossdip stack, the upper crust is schematically divided into three regions by a dashed blue line. Region I is composed of greenstones. Region II is composed of intrusions that crop out south of the seismic line (see Fig. 3). Region III is the top of the basement complex. (b, c) Three-dimensional prestack migration. (b) An isosurface presentation of the image data of the strongly negative intensities with two variable density slices as background. Events A, B, C, and D are the same as in Figure 6a. (c) Isosurface and data slice view of strong events in the southwestern part of the near-surface data volume.

have a discordant relationship with the basement structure (Fig. 6a).

Similar to rocks in other greenstone belts, metavolcanic rocks at Sturgeon Lake have steep stratigraphic dips. Since most of the bedrock in the area is covered with Quaternary sediments of glacial origin, the most complete bedrock-dip information comes from the regions where ore was explored for or mined. Strata in the Mattabi mine area dip at angles between 65° and 85° (Franklin et al., 1975). In the Lyon Lake deposit area, they dip at 50° to 70° north in the north-south mine sections (Harvey and Hinzer, 1981). Because the contacts strike between 95° and 120° azimuth, the true structural dips are somewhat larger. The profile of the Sturgeon Lake deposit presented by Severin (1982) features strata that dip in the range from 50° to 90°. Bedding at a large bedrock outcrop ~1,500 m south of the Lyon Lake deposit dips at 80°. Such steep dips at shallow depth are beyond the limit of what modern reflection methods can image when the final product is a stacked two-dimensional section. This is confirmed in the optimum crossdip stack where no steep events are imaged in the upper kilometer (i.e., to ~0.35 s). At a greater depth (greater than about 1.5 km $\simeq$ 0.5 s), the image is believed to be reliable.

We believe that the regions defined in Figure 6a record major elements of the upper crust in the study area. Region I corresponds to greenstones estimated to have a maximum depth of 2.7 to 3.0 km. Gravity modeling done much earlier by Dusanowskyj (1976) also set the maximum depth of the greenstones at ~3.0 km. The two results closely agree. Region II is believed to be composed of intrusions that are either closely related to the Beidelman Bay pluton, Southern granitic complex, and Bell Lake alkalic complex, or represent their subsurface roots. Region III is the basement complex, only the top part of which has been imaged.

Migrated images

The seismic procedure most capable of imaging steeply dipping reflectors is three-dimensional prestack migration. This process requires an enormous amount of central processing unit (CPU) power, and it represents a great challenge even for fast workstations. In order to reduce the migration run-time, we reduced the size of the desired initial output volume to 9.7 km × 6.0 km × 6.0 km (length × width × depth; Fig. 7) and set an 18 m output sample spacing in all three directions. To prevent aliasing (signal distortion owing to undersampling), we migrated signal only to ~90 Hz. Further reduction in migration run-time was achieved by a partial stack of the input data traces in the common midpoint bin gathers. Because of the partial stacking, reflections from steeply dipping interfaces in the uppermost kilometer are not expected to be well handled. Figure 6b shows an isosurface and slice image of the main events in the initial volume. Isosurface images are colored and shaded constant-amplitude surfaces (of strong negative seismic amplitude, in our examples). Image slices are sectional planes on which seismic amplitude is displayed as color or in grayscale. Both are extracted from a three-dimensional image volume.

The majority of the imaged reflection events migrate south from the northeast-southwest processing and acquisition line where they display an east-west strike and a northerly dip (Figs. 6b and 8). The strongest groups of events are labeled A, B, C, and D and correspond to the similarly labeled events in the optimum crossdip stack of Figure 6a. The two approaches yield results that agree with each other. Moreover, the location and attitude of reflector groups A, B, C, and D is much easier to visualize in the three-dimensional volume (Fig. 6b), and that figure further clarifies their close relationship with the intrusive rock units shown on the geologic map in Figures 3 and 7.

Despite our reservations about migrating partially stacked data, we were able to observe two sets of events in the shallow part of the initial data volume. One is a steeply dipping reflective structure in the contact zone between the Beidelman Bay pluton and the greenstones; the other is a northward-dipping structure close to the zone of economic interest. This observation led us to design two smaller output data volumes (detail 1 and detail 2 in Figs. 7, 9, and 10) in which the full frequency range of the recorded signal (to 300 Hz) and the original traces could be exploited. To prevent signal aliasing, we set the output grid much denser (5 m). However, because we were interested only in the very shallow structure, we were able to limit the input data travel times to 1 s and offsets to ±1 km.

We also reran the migration for the top 1.5 km of the area near the processing line (cross-line offsets of ±750 m) to obtain what we call the near-surface data volume (see Fig. 7 for its outline). Since this image volume is very large, we set the sampling in the output grid to 10 m and were able to migrate the signal only to ~165 Hz. As in the migration of detail 1 and 2 volumes, no partial stacking was applied to the input traces, travel times were limited to 1 s, and offsets to ±1 km.

Near-surface volume: Numerous reflectors are visible under kilometers 5 to 6 of the processing line (Fig. 6c). They dip northward and are situated at depths greater than about a half kilometer. Direct correlation of the observed reflectors with specific surface geologic contacts is difficult because of the reflector depth and because the imaged parts of the reflectors are not very extensive. However, on the basis of the reflector projections to the surface, they probably originate within the intermediate metavolcanic rocks of formation B or at the boundary between formation A and B of volcanic cycle 1. The detail 1 volume partially overlaps this volume (Fig. 7).

The very large circular arc is most likely an artifact or exaggeration. The recording line is too straight in this part of the survey to permit the reflector to be positioned unambiguously in space. The true reflection area on the arc is near the other north-dipping events.

Detail 1 volume: Figure 9 shows the surface area covered by the detail 1 volume (Fig. 11a). A thick band of strong, north-dipping (azimuth ~5°) reflections is observed. On the basis of both the position of the reflection band in the image volume and a detailed knowledge of the surface geology, we believe that these reflections originate within the precaldera volcanic rocks that are known to be heterogeneous. The strongest reflections within the band most likely occur at the boundaries between interlayered mafic and felsic flows. At deeper levels, the precaldera reflection events are stronger and less steep, and they form a thicker reflection band.

The boundary between the precaldera volcanic rocks and the Beidelman Bay pluton also appears to be sharp. In Figure

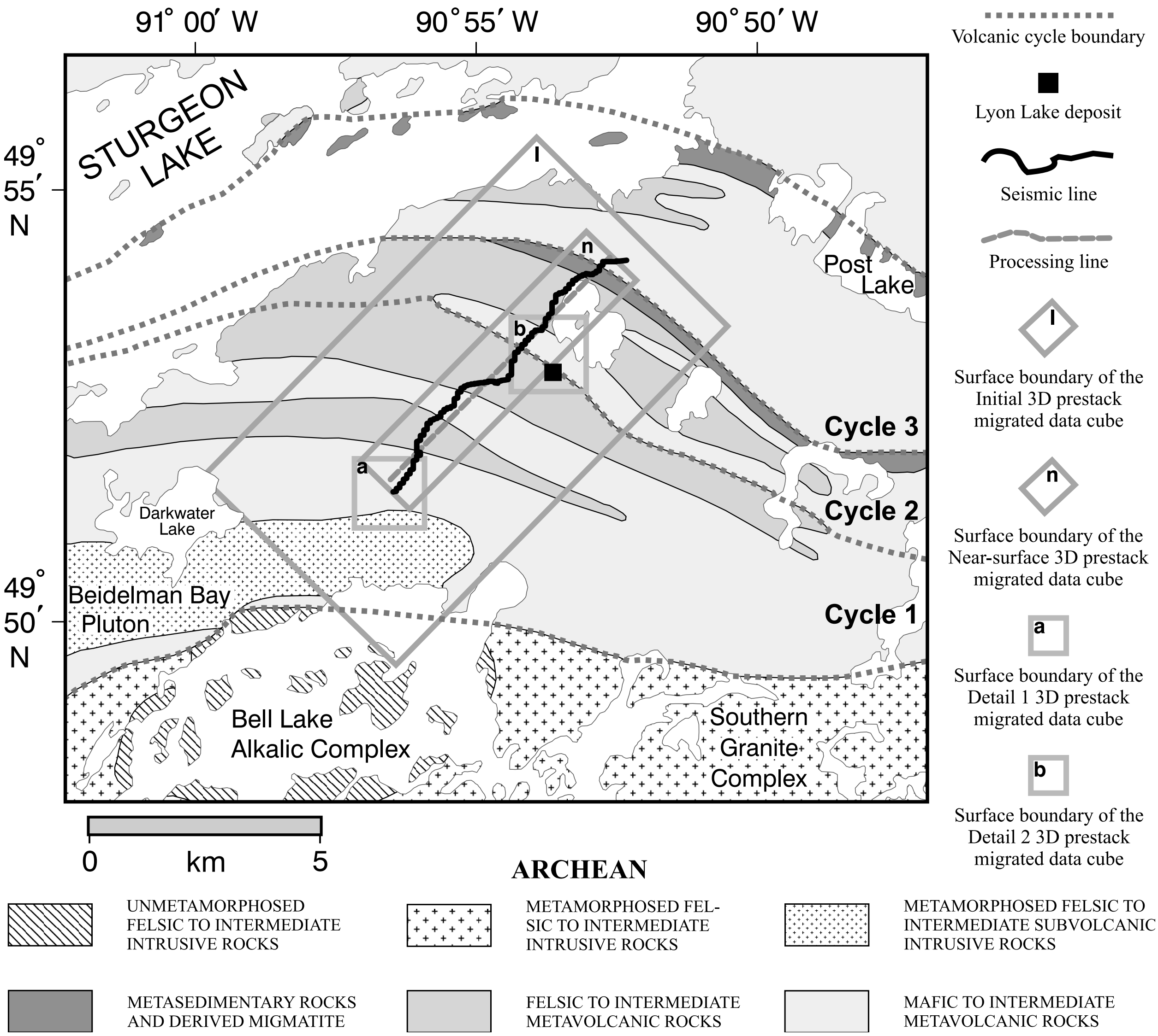

FIG. 7. Simplified geologic map from Figure 3 showing the surface location of the migrated data volumes. Processing for the initial and near-surface data volumes was designed to image only large-scale structures. Processing for the detail 1 and detail 2 data volumes was designed for detailed imaging.

11a, it is represented by a sudden drop in reflection amplitudes, and it dips very steeply toward the north and projects to the surface contact between the greenstones and the intrusion. Reflection events in the Beidelman Bay pluton are weaker and steeper than in the greenstones. The relatively weak and steeply dipping reflections that originate within the Beidelman Bay pluton and the upper 400 m of the precaldera volcanic rocks do not necessarily reflect on the lithology. The weakness of these reflections may be due to the inability of the seismic method to image in full strength the very shallow steep events, or it may be due to the viewpoint limitation.

Immediately overlying the precaldera metavolcanic rocks is the mesobreccia unit of the High Level Lake succession. Because the mesobreccia unit is a pile of poorly sorted deposits composed of block and lapilli-size clasts of mafic and felsic volcanic rocks, it scatters reflection energy. Consequently, at the northern upper end of the image slice in Figure 11a, the mesobreccia unit is represented by weak and discontinuous subhorizontal events.

Detail 2 volume: Of the several base-metal massive sulfide deposits discovered in the southern Sturgeon Lake assemblage, only the structure surrounding the Lyon Lake deposit appears close enough and favorably enough oriented to be imaged by the seismic reflection profile. The detail 2 image volume was therefore approximately centered at this deposit (Fig. 10). Figure 11b and c display the results for depths above and below 1 km.

Figure 11b shows a vertical image slice through the Lyon Lake deposit at an azimuth of 23°. Despite the appreciable level of background noise owing to imperfections of the migration procedure and the acquisition geometry, a pervasive suite of steeply north-dipping reflections is clearly seen to

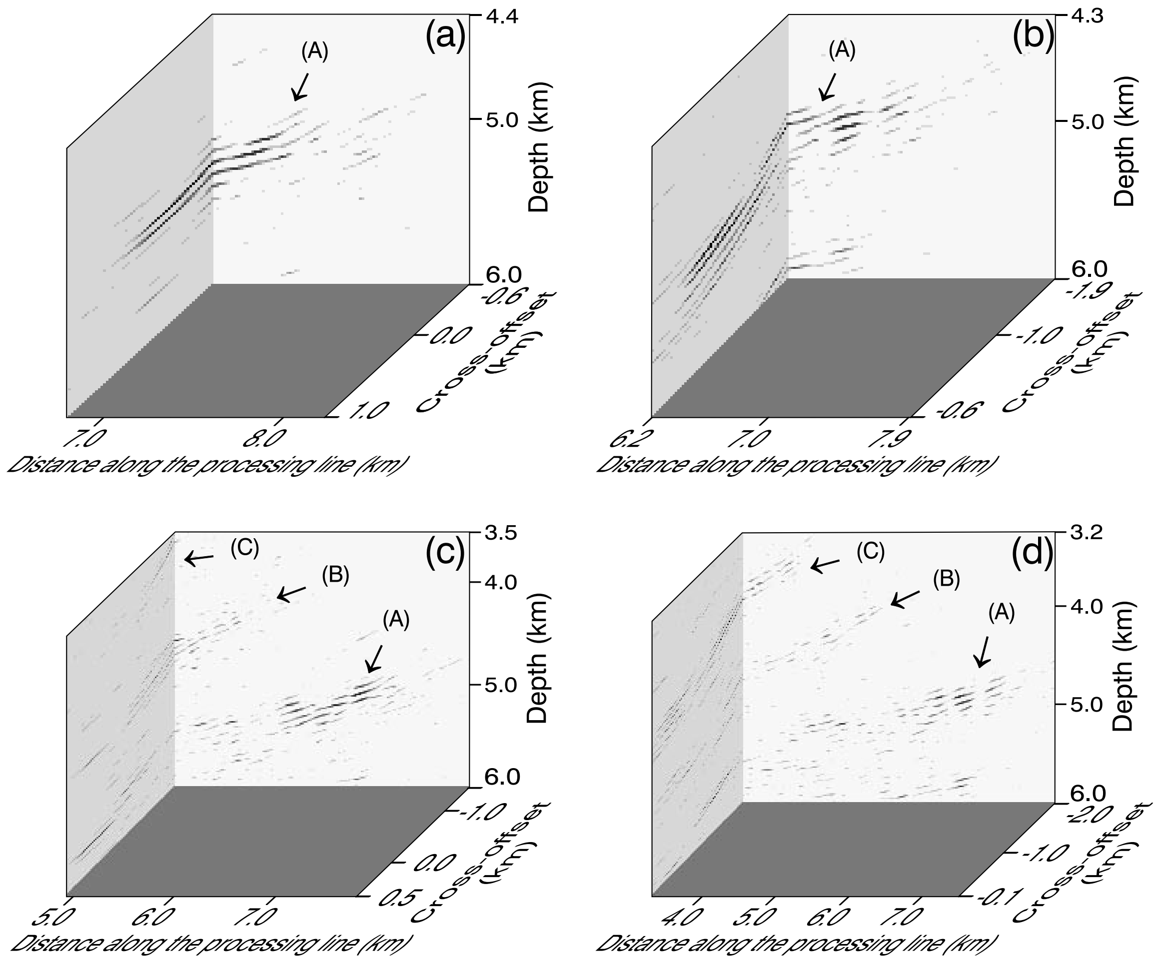

FIG. 8. Closeups of the strongest groups of events in the initial three-dimensional prestack migrated volume of Sturgeon Lake line data: (a, b, c, d) Perspective views from the west of vertical variable density sections through event groups A, B, and C parallel and perpendicular to the processing line. The labeled reflectors clearly exhibit both in-line and cross-line dip. Views (a) and (b) are zoomed more than views (c) and (d).

within 100 m of the surface. Although changes in reflection amplitude and character are not sharp, three distinct groups of reflections can be recognized and are labeled A, B, and C.

Group B events are the most continuous. The location and surface projection of the stratigraphically lower reflectors in this group coincides with the boundary between volcanic cycles 1 and 2. In the transected area, this boundary is represented by the contact between the overlying basaltic-andesitic rocks of the Lyon Lake andesite (Trowell's formation F) and the underlying pyroclastic deposits of the L succession (Trowell's formation E). The cycle 1 and 2 boundary is also the locus of the massive sulfide deposits and, according to Dubé et al. (1989) and J. Franklin (pers. commun., 2002), it is a thrust fault manifested by a zone of high strain (high schistosity) that is thickest in the hanging-wall unit (~100 m). The fault, the orebodies, and the enclosing rocks show later penetrative deformation that has produced wavy ramp-flat structures, so the regional northward dip is not uniform locally. With increasing depth, the fault departs very gently from the dip of the strata.

It seems likely that the stratigraphically upper and middle reflection events in group B are due to the observed interlayering between the massive to amygdaloidal basalt-andesite sheet flows, pillow lavas, hyaloclastites, and scoriaceous rocks of the hanging wall formation F. The dip of the group B events slightly flattens below 0.7 km but remains close to the range 50° to 55° known from drilling (Harvey and Hinzer, 1981).

The surface projection of the group A reflectors correlates well with the contact between the above-described Lyon Lake basalt-andesite flows (Trowell's formation F) and the overlying massive felsic effusive rocks of the Swamp Lake succession (Trowell's formation G). In the top 500 m, group A events dip at approximately 60°. Below this, the dip moderates to ~45° and then to ~35°. The moderation of structural dip with increasing depth, as suggested by the geometry of reflection groups A and B, is probably due to regional folding, and it is consistent with the apparent thickening of the hanging wall units observed at the surface (J. Franklin, pers. commun., 2002).

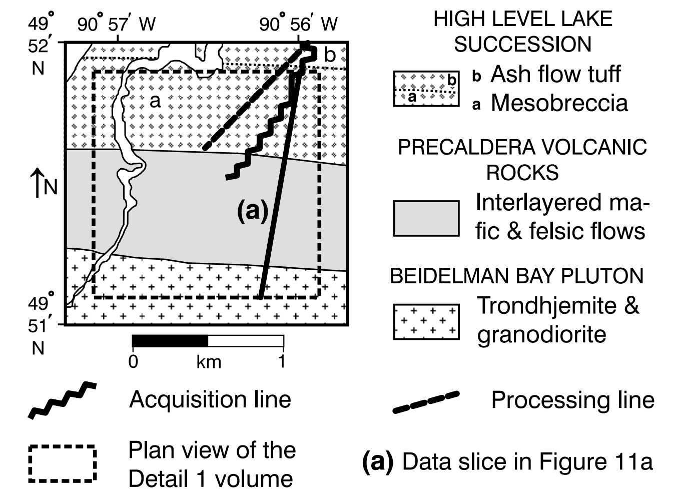

FIG. 9. Surface area of the detail 1 volume (1.5 × 1.5 × 1.2 km) chosen for a full signal (10–300 Hz) three-dimensional prestack migration. The solid straight line is the surface trace of the vertical image slice shown in Figure 11a. The underlying geology is based on Morton et al. (1996) and Ontario Geological Survey Map 2457 (1981).

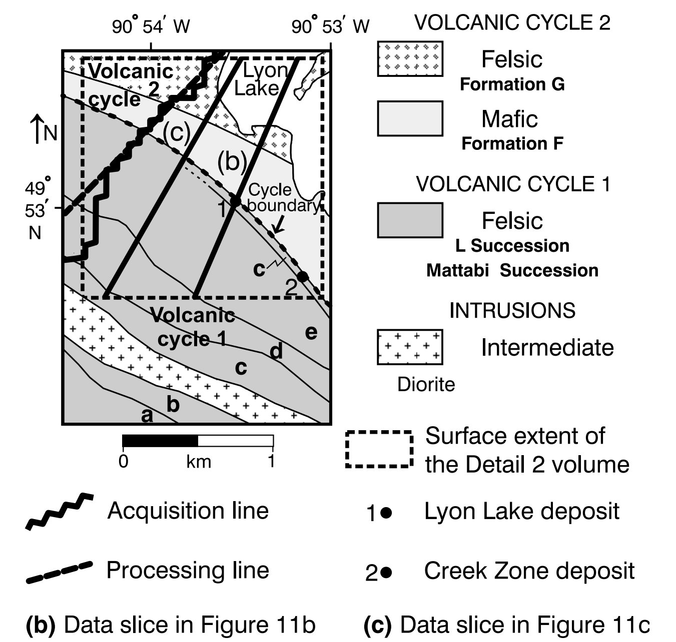

FIG. 10. Surface area of the detail 2 image volume (1.6 × 1.6 × 2.0 km). The surface traces of the vertical slices displayed in Figures 11b and 11c are shown by the two solid straight lines. The underlying geology is based on Morton et al. (1996) and Ontario Geological Survey Map 2457 (1981). Formation G is composed of lapilli-tuff, lapillistone tuff, and quartz-feldspar porphyry intrusions. Formation F is composed of interlayered massive to amygdaloidal, basaltic-andesitic sheet flows, pillow lavas, hyaloclastites, and scoriaceous rocks. The L succession comprises unit e (Lyon Lake dacitic lava dome complex, associated sediments and debris flow deposits); unit d (lava flows, volcaniclastic sediments, debris flow deposits); unit c (middle and upper L pyroclastic deposits); unit b (lower L pyroclastic deposits). The Mattabi succession consists of unit a (pyroclastic flow deposits).

Events of group C in the southern end of the image slice also dip steeply (~55º). Their surface projection correlates well with the pyroclastic unit c in the L succession (Fig. 10), that crops out about 200 m southwest of the image slice. In this area (within unit c), the pyroclastic deposits are interlayered with lava flows, volcaniclastic sediments, and debris flow deposits of unit d (Morton et al., 1996). This interlayering is the likely cause of group C reflection events.

The area between group C and group B events on the image slice of Figure 11b gives the weakest and least continuous reflections. It projects to the surface at the units d and e of the L succession (Fig. 10). These units are not homogeneous, and the reason for the low reflectivity is not obvious. Perhaps the lithologic contacts are rough surfaces that scatter the wave energy instead of reflecting it.

Figure 11c shows the strongest reflection events in the image volume. They are situated west of the Lyon Lake deposit in the deeper part of the migrated data volume (1,300–1,600 m), have gentle north-northeast dips (~5º–25º), strike at ~120º, and may outline flattened zones in the regional fold structure. Another group of weaker and generally steeper reflections (~20º–40º) is marked by dashed green lines in the image slice. According to their projection, they may be related to the contact between the diorite intrusion and the surrounding lower and middle L succession pyroclastic deposits of volcanic cycle 1. Both contacts reach the surface southwest of the detail 2 data area (Fig. 10) and there strike at about 120º.

A thrust slice composed of unit c quartz-rich pyroclastic flows are the host rocks for the Lyon Lake and Creek Zone massive sulfide deposits (Fig. 10). These orebodies were tectonically deformed and apparently transported westward from the Sturgeon Lake orebody along the thrust fault separating cycle 1 and cycle 2 (Franklin et al., 1977; J. Franklin, pers. commun., 2002). The Lyon Lake deposit is a sheet-like orebody, 300 to 320 m long and approximately 10 m thick, conformable with the surrounding formations. Its position is indicated on the image slice in Figure 11b according to the information provided in Harvey and Hinzer (1981). Since reflections are pervasive, it is difficult to associate the orebody with any specific reflector. Geologic layering in the area is thin and highly developed, and it has many potential contacts of strong reflectivity. Furthermore, the orebody is not a plain, steeply dipping flat sheet. Parts of the Lyon Lake orebody lie on horizontal or gently dipping segments of a local fold and are structurally thickened (Dubé et al., 1989). These shallowly plunging structures are not oriented favorably to be imaged by the survey, and they could, in part, have caused the local discontinuities observed within the steeply dipping reflections of group B. Finally, the thickness of the orebody is less than a quarter wavelength of the seismic data for frequencies below about 140 Hz. This relationship implies that higher resolution and higher frequency two-dimensional data acquired along the structural-dip line may be required to directly image the orebody.

Discussion and Conclusions

We have processed the Sturgeon Lake seismic reflection survey data by applying both the standard two-dimensional common midpoint imaging methodology and two recently

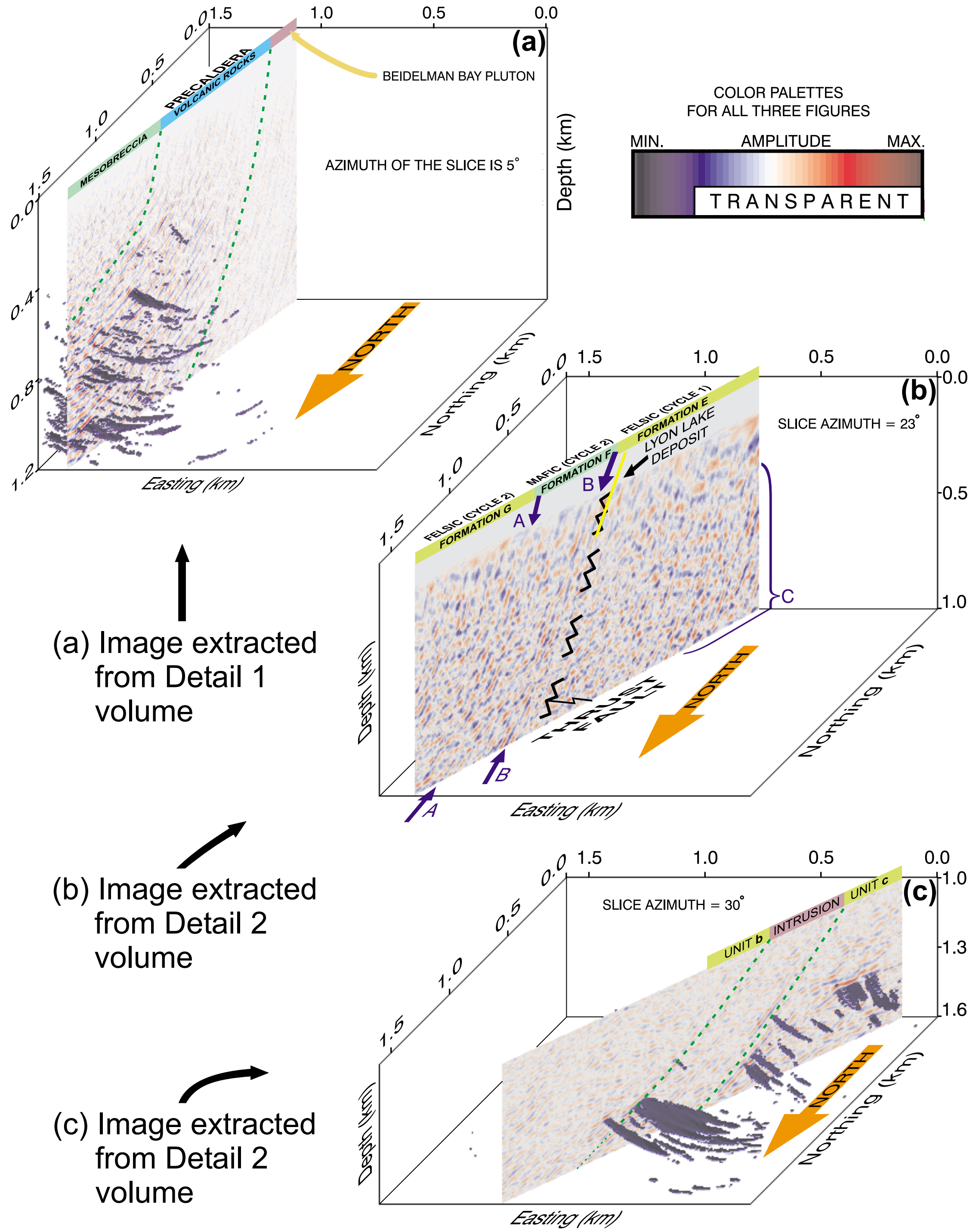

FIG. 11. Detailed images obtained by three-dimensional prestack migration of the shallow seismic data (locations in Figures 7, 9, and 10). (a) Isosurface and image slice view of the detail 1 data volume showing reflectors in the contact zone between the Beidelman Bay pluton and the metavolcanic rocks of cycle 1. (b, c) Three-dimensional prestack migration of the detail 2 data volume near the Lyon Lake deposit. (b) Image slice crossing the Lyon Lake deposit. The surface positions of contacts between formations E, F, and G are indicated. The position of the Lyon Lake deposit is shown on the image slice. Blue arrows and brackets indicate the locations of reflection groups A, B, and C. Group A reflections occur at the contact between the Lyon Lake basalt-andesite flows (formation F) and the felsic rocks of the Swamp Lake succession (formation G). Upper and middle group B events are due to the interlayering of basalt-andesite sheet flows and other rocks of formation F. Lower group B reflections originate at the boundary of volcanic cycles 1 and 2, which is also a major thrust fault. Group C events are due to interlayering of felsic rocks of units c and d, L succession (formation E). (c) Isosurface and image slice view of the strongest and most continuous reflectors in the detail 2 volume. Pyroclastic deposits of units b and c surround the intermediate intrusion. Dashed green lines in (a) and (c) indicate the approximate subsurface position of the surficially mapped geologic contacts.

designed procedures for extracting three-dimensional structural information from two-dimensional crooked line data. The resulting two-dimensional sections, the standard stack and the optimum crossdip stack, display similar patterns of strong reflectivity below about 0.5 s travel time (1.5 km depth). However, the optimum crossdip stack improved the imaging of these deep reflections and provided some three-dimensional positional information about them, permitting a geologic interpretation. The uppermost parts of both sections are unreliable, and they cannot be used to connect the imaged reflectors with the known surface geology. Only the three-dimensional prestack migration allowed elucidation of the shallow structure.

The highest resolution three-dimensional migrations (details 1 and 2) clearly show several bands of reflectors that correlate very well with the known volcanic stratigraphy of the south Sturgeon Lake assemblage. The limited cross-profile aperture of the survey generally was sufficient to position the reflectors with reasonable accuracy. However, migration noise that resulted in artifacts was commonly present. At the southwest end of the profile, it appears that the contact between the greenstones and the Beidelman Bay pluton has been imaged. Potential ore-controlling structures in close vicinity of the Lyon Lake deposit are imaged, and possibly the ore zone itself, confirming that it is possible to extract useful three-dimensional reflection images from the shallow part of two-dimensional crooked line survey data.

The viewpoint limitation of any two-dimensional survey seriously limits what can be imaged. When two-dimensional crooked line data from a generally monoclinal assemblage such as this example are processed by three-dimensional prestack migration, reflection points are roughly confined to a small part of the three-dimensional image volume defined by the formation attitudes and the geometry of the survey line. Away from this part, there is little information in the image volume. It is essential to retain high frequencies (300 Hz) in the data in order to have useful resolution at the mineral exploration scale. A sufficient number of traces with sufficient aperture in the in-line and cross-line directions are required to position the reflection points adequately. Basically, surveys should be designed to proceed directly to prestack migration, instead of common midpoint stacking. Reflections in this data set were strong enough and coherent enough that it was not necessary to combine large numbers of traces with a wide range of offsets and azimuths (i.e., to have a large survey fold) to produce good images. This lack of a need for a large survey fold suggests that it may be possible to design relatively simple and relatively inexpensive survey geometries for full three-dimensional imaging of structures in crystalline rocks, especially if the structural trends can be approximately predicted in advance.

Acknowledgments

This research was partly supported by grants from the Natural Sciences and Engineering Research Council of Canada to G.F. West and by U.S. Geological Survey National Earthquake Hazards Reduction Project (NEHRP) funds awarded to R.D. Hyndman. The Sturgeon Lake line data, drill hole logs, and summary of descriptive core logs were generously provided by Larry Petrie, Larry Matthews, and Al Smith of Noranda Inc. We acknowledge the financial support of the Ontario Geological Survey in the conduct of the survey. The Geological Survey of Canada-Pacific, where this paper was written, financially supported its publication. We are also grateful to Mark Hannington, James Franklin, Christopher Juhlin, and Suzanne Paradis for their reviews, which have significantly improved the manuscript.

June 20, 2001; July 16, 2002

REFERENCES

Blackburn, C.E., Johns, G.W., Ayer, J., and Davis, D.W., 1991, Wabigoon subprovince, *in* Geology of Ontario: Ontario Geological Survey Special Volume 4, Part I, p. 303–382.

Campbell, I.H., Franklin, J.M., Gorton, M.P., Hart, T.R., and Scott, S.D., 1981, The role of subvolcanic sills in the generation of massive sulfide deposits: ECONOMIC GEOLOGY, v. 76, p. 2248–2253.

Campbell, I.H., Coad, P., Franklin, J.M., Gorton, M.P., Scott, S.D., Sowa, J., and Thurston, P.C., 1982, Rare earth elements in volcanic rocks associated with Cu-Zn massive sulfide mineralization: Canadian Journal of Earth Sciences, v. 19, p. 619–623.

Clowes, R.M., Cook, F., Hajnal, Z., Hall, J., Lewry, J., Lucas, S., and Wardle, R., 1999, Canada's Lithoprobe project (collaborative, multidisciplinary geoscience research leads to new understanding of continental evolution): Episodes, v. 22, p. 3–20.

Davis, D.W., Krogh, T.E., Hinzer, J., and Nakamura, E., 1985, Zircon dating of polycyclic volcanism at Sturgeon Lake and implications for base metal mineralization: ECONOMIC GEOLOGY, v. 80, p. 1942–1952.

Davis, D.W., Sutcliffe, R.H., and Trowell, N.F., 1988, Geochronological constraints on the tectonic evolution of a late Archean greenstone belt, Wabigoon subprovince, northwest Ontario, Canada: Precambrian Research, v. 39, p. 171–191.

Dubé, B., Koopman, E.R., Franklin, J.M., Poulsen, K.H., and Peterson, M.R., 1989, Preliminary study of the stratigraphic and structural controls of the Lyon Lake massive sulphide deposit, Wabigoon subprovince, northwestern Ontario: Geological Survey of Canada Current Research Part C, paper 89-1C, p. 275–284.

Du Bois, L., Levato, L., Escher, A., Marchant, R., Oliver, R., Ouwehand, M., Sellami, S., Steck, A., and Wagner, J.J., 1990, Pseudo-3D study using crooked line processing from the Swiss Alpine western profile—Line 2 (Val d'Anniviers-Valais): Tectonophysics, v. 173, p. 31–42.

Dusanowskyj, T.H., 1976, A gravity study of the Sturgeon Lake metavolcanic-metasedimentary belt: M.Sc. thesis, University of Toronto, Ontario, 75 p.

Franklin, J.M., 1996, Volcanic-associated massive sulphide base metals, *in* Eckstrand, O.R., Sinclair, W.D., and Thorpe, R.I., eds., Geology of Canadian Mineral Deposit Types: Geological Survey of Canada, The Geology of Canada, no. 8, p. 158–183 (also Geological Society of America, The Geology of North America, v. P-1).

Franklin, J.M., Kasarda, J. and Poulsen, K.H., 1975, Petrology and chemistry of the alteration zone of the Mattabi massive sulfide deposit: ECONOMIC GEOLOGY, v. 70, p. 63–79.

Franklin, J.M., Gibb, W., Poulsen, K.H., and Severin, P., 1977, Archean metallogeny and stratigraphy of the south Sturgeon Lake assemblage: Institute on Lake Superior Geology Annual Meeting, 23rd, Mattabi field trip guidebook, 73 p.

Galley, A., van Breemen, O., and Franklin, J. M., 2000, The relationship between intrusion-hosted Cu-Mo mineralization and the VMS deposits of the Archean Sturgeon Lake mining camp, northwestern Ontario: ECONOMIC GEOLOGY, v. 95, p. 1543–1550.

Groves, D.A., Morton, R.L., and Franklin, J.M., 1988, Physical volcanology of the footwall rocks near the Mattabi massive sulphide deposit, Sturgeon Lake, Ontario: Canadian Journal of Earth Sciences, v. 25, p. 280–291.

Harvey, J.D., and Hinzer, J.B., 1981, Geology of the Lyon Lake ore deposits, Sturgeon Lake area, Ontario: The Canadian Institute of Mining Bulletin, v. 74, p. 77–84.

Juhlin, C., 1990, Interpretation of reflections in the Siljan ring area based on results from the Gravberg-1 borehole: Tectonophysics, v. 173, p. 345–360.

Kim J., Moon, W.M., Percival, J.A., and West, G.F., 1992, Seismic imaging of shallow reflectors in the eastern Kapuskasing structural zone, with correction of cross-dip attitudes: Geophysical Research Letters, v. 19, p. 2035–2038.

Larner, K.L., Gibson, B., Chambers, R., and Wiggins, R.A., 1979, Simultaneous estimation of residual statics and crossdip time corrections: Geophysics, v. 44, p. 1175–1192.

Milkereit, B., Berrer, E.K., King, A.R., Watts, A.H., Roberts, B., Eaton, D.W., Wu, J., and Salisbury, M.H., 2000, Development of 3D seismic exploration technology for nickel-copper deposits: A case history from the Sudbury basin, Canada: Geophysics, v. 65, no. 6, p. 1890–1899.

Morton, R.L., Walker, J.S., Hudak, G.J., and Franklin, J.M., 1991, The early development of an Archean submarine caldera complex with emphasis on the Mattabi ash-flow tuff and its relationship to the Mattabi massive sulfide deposit: ECONOMIC GEOLOGY, v. 56, p. 1002–1011.

Morton, R.L., Hudak, G., and Koopman, E., 1996, Physical volcanology, hydrothermal alteration and massive sulphide deposits of the Sturgeon Lake Caldera: Geological Association of Canada/Mineralogical Association of Canada Annual Meeting, Winnipeg, Manitoba, 1996, Field Trip Guidebook B3, 37 p.

Nedimović, M.R., and West, G.F., 1999, Processing seismic reflection data from high fold, crooked line surveys in crystalline geological terrain: International Meeting of the Society of Exploration Geophysicists, 69th, Houston, Texas, 1999, Expanded abstracts, p. 1437–1440.

——2000, Migrating 2D crooked line seismic reflection data from crystalline geological terrain: International Meeting of the Society of Exploration Geophysicists, 70th, Calgary, Canada, 2000, Expanded abstracts, p. 894–897.

Nedimović, M.R., Wang, W., and West, G.F., 1998, Focusing problems in reflection imaging of the crust: International Symposium on Deep Seismic Profiling of the Continents and Their Margins, 8th, Barcelona, Spain, 1998, Abstracts, p. 42.

Ontario Geological Survey, 1980, Sioux Lookout-Armstrong, *in* Kenora and Thunder Bay districts, Geological Compilation Series: Ontario Geological Survey Map 2442, scale 1:253,440.

——1981, Sturgeon Narrows, *in* Precambrian Geology: Ontario Geological Survey Map 2457, scale 1:50,000.

Pretorius, C.C., Trewick, W.F., Fourie, A., and Irons, C., 2000, Application of 3D seismics to mine planning at Vaal Reef's gold mine, no. 10 shaft, Republic of Southern Africa: Geophysics, v. 65 no. 6, p. 1862–1870.

Severin, P.W.A., 1982, Geology of the Sturgeon Lake copper-zinc-lead-silver-gold deposit: The Canadian Institute of Mining Bulletin, v. 75, p. 107–122.

Trowell, N.F., 1974, Geology of the Bell Lake-Sturgeon Lake area, districts of Thunder Bay and Kenora: Ontario Geological Survey Report 114, 67 p.

——1983, Geology of the Sturgeon Lake area, Districts of Thunder Bay and Kenora: Ontario Geological Survey Report 221, 97 p. Accompanied by Ontario Geological Survey Maps 2456, 2457, and 2458, scale 1:50,000; 1 chart, and 1 sheet of microfiche.

Trowell, N.F., Blackburn, C.E., Edwards, G., and Barlett, J.R., 1980, Preliminary geological synthesis of the Savant Lake-Crow Lake metavolcanic-metasedimentary belt, northwestern Ontario, and its bearing upon mineral exploration: Ontario Geological Survey Miscellaneous Paper 89, 30 p.

Wang, W., and West, G.F., 1991. Stacking processes of crooked lines using the SUN/INSIGHT system: Lithoprobe Seismic Processing Facility Newsletter, v. 4, p. 13–18.

White, D.J., Forsyth, D., Nedimović, M. R., Perron, G., Carroll, P., van der Valden, A., Hall, K., and Harrap, R., 1997, Seismic reflection data acquisition in the western Superior transect: University of British Columbia Lithoprobe Secretariat, Lithoprobe Report 65, p. 79.

APPENDIX

Data Processing

Processing was carried out in three stages. The first stage was standard two-dimensional crooked line processing to create common midpoint bin gathers, corrected for normal moveout and in-line dip moveout. The second and third stages consisted of the optimum crossdip stacking procedure and the three-dimensional prestack migration procedure described by Nedimović and West (1999, 2000). In the second stage, data traces from step one were corrected for crossdip moveout on the basis of a local semblance analysis, and finally stacked to form the two-dimensional optimum crossdip stack. The optimum crossdip stack image includes the three-dimensional information about structures extracted by the crossdip moveout analysis. For the third stage, original data traces were locally averaged (partially stacked), and then the prestack migrated directly into a three-dimensional image of reflectivity. The initial step of partial stacking was optimized for the full 3 s of data and resulted in a poorer image at shallow depths. Therefore, the uppermost 1.5 s of data were prestack migrated into three-dmensional image volumes before any partial stack was applied.